Article

Effect of Absorption Time for the Preparation of Activated Carbon from Wasted Tree Leaves of *Quercus alba* and Investigating Life Cycle Assessment

Muhammad Amin [1,*] **and Hamad Hussain Shah** [2]

1   Department of Energy Systems Engineering, Seoul National University, Seoul 08826, Korea
2   Department of Engineering, University of Sannio, Piazza Roma 21, 82100 Benevento, Italy
*   Correspondence: aminshoukat3333@yahoo.com

Abstract: In this article, the effect of absorption time on the surface chemistry and pore structure of activated carbon (AC) from waste leaves of *Quercus alba* with the H_3PO_4 chemical activation method. XRD, SEM, EDX, BET, TGA, and FT-IR analyses of prepared AC were used to figure out the properties of the activated carbon. The results demonstrated that the 48 h absorption time of H_3PO_4 contributed to the highest surface area, 943.2 m^2/g, among all the prepared activated carbon samples. As the absorption time of the phosphoric acid activating agent was increased, the surface area initially increased and then started to decrease. The further surface chemical characterization of activated carbon was determined by FT-IR spectroscopic method. Life cycle assessment methodology was employed in order to investigate the environmental impacts associated with the laboratory steps for activated carbon (AC) production. The LCA approach was implemented using OpenLCA 1.10.3 software, while ReCiPe Midpoint (H) was used for environmental impact assessment. The results of the LCA study showed that the impact categories related to toxicity were particularly affected by the utilization of electrical energy (≈90%). The power utilized during laboratory procedures was the main cause of environmental impacts, contributing an average of nearly 70% across all impact categories, with the maximum contribution to the impact category of freshwater ecotoxicity potential (≈97%) and the minimum contribution to land use potential (≈10%).

Keywords: *Quercus alba*; activated carbon; absorption time; life cycle assessment

1. Introduction

Quercus alba (white oak) is a long-lived shaded tree normally found in eastern Canada and some parts of the United States that grows up to 100 feet. *Quercus alba* is one of the preeminent hardwoods of eastern North America [1,2]. Because of its ability to grow in a variety of climatic regimes, it is found not only in North America but also in Asia. In India, more than 16 species of oak are present, out of which 10 are present in the eastern Himalayas, and the rest of them are found in the western Himalayan regions [3]. *Quercus alba* has been utilized in various wood-oriented industries, including the cooperage industry, forest aesthetics, and wildlife. In addition, *Quercus alba* can be used for the preparation of activated carbon (AC). There are numerous biomass sources available for the preparation of AC, but the most commonly used are corn straw [4], Christmas trees [5], almond shells [6], walnut shells [7], coconut shells [8], pomegranate peels [9], Lantana camara [10,11], olive tree leaves [12], and many more [13]. Among all these waste biomass sources, the leaves of *Quercus alba* are abundantly available as a waste biomass source. Activated carbon with an enormous surface area is frequently used in industries as an adsorbent [14], for catalysis purposes [15], and in other important applications. Figure 1 shows the use of activated carbon for various applications.
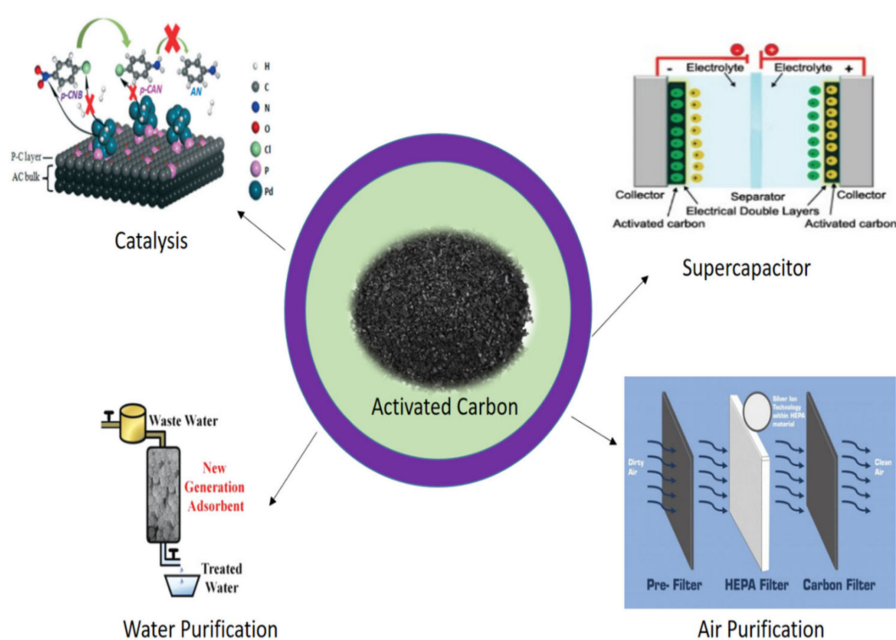
Figure 1. Use of activated carbon in various applications.

Activated carbon can be produced from biomass by the thermal process through direct carbonization or by first carbonizing the biomass to biochar and later converting the biochar into activated carbon [16]. Activated carbon is generally produced by chemical or physical activation methods. In the physical activation method, the process is performed under the circumstances of an inert atmosphere, and pyrolysis of carbonaceous material is performed at a high temperature to eliminate most of the hydrogen and oxygen content [17]. The chemical activation process involves carbonization at a low temperature of 400–700 °C with a chemical activation agent [18]. Biomass or wood wastes are often used to produce activated carbon in the chemical activation process [19]. Different activation agents have different effects on the thermal degradation of the organic compounds in biomass. To date, many activation agents, such as H_3PO_4, $ZnCl_2$, $FeCl_3$, KOH, H_2SO_4, and many more, have been used for the preparation of activated carbon [20]. Among these, H_3PO_4 is used the most frequently. The H_3PO_4 activating agent increases the surface area of activated carbon and increases the number of defects of the anchoring site for metal particles [21]. H_3PO_4 oxidizes carbon particles at 500–600 °C to create micropores [22] and has the advantage of inhibiting the shrinkage of particles with a low operating cost.

The important factors for the preparation of AC are the raw biomass source, activation method, activation agent, impregnation ratio, concentration of the activated agent, absorption time of the activation agent, and calcination temperature. The surface area of AC is significantly influenced by all the above parameters [23]. The first aim of this study was to determine the effect of the absorption time of the activation agent (H_3PO_4) on the preparation of activated carbon from waste leaves from *Quercus alba*.

Life cycle assessment (LCA) is a methodological approach used to evaluate processes' environmental impacts. There are generally four stages of LCA: (i) goal and scope definition, (ii) life cycle inventory (LCI), (iii) life cycle impact assessment (LCIA), and (iv) interpretation. Few studies have been published regarding the ecological assessment of AC production by utilizing the LCA approach. Arena et al. [24] and Tagne Tiegam et al. [25] assessed the environmental impacts of producing AC from coconuts shells and cocoa pods. The authors found that during AC production, the consumption of energy and the chemical activation stage caused most of the environmental damage. By using sustainability factors assessed through LCA, a quantitative optimization approach was developed by Sepúlveda-Cervantes et al. for efficient AC production to reduce the environmental impacts associated with the production process using soybean shells as the precursor [26,27].

Therefore, the second aim of this study was to assess the environmental impacts associated with the conversion process of waste leaves of *Quercus alba* into activated carbon and to assess the key variables that affect activated carbon production. The overall objective of the current study was to overcome the information gap related to the environmental impacts of producing activated carbon from *Quercus alba*.

2. Materials and Methods

2.1. Chemicals

Distilled water and phosphoric acid (Sigma-Aldrich, St. Louis, MO, USA, initial concentration 85% and density 1.68 g/mL) were purchased from a local market in Seoul, Republic of Korea. The waste leaves of *Quercus alba* were collected from Seoul National University.

2.2. Activated Carbon Preparation Procedure

Fallen waste leaves of *Quercus alba* contain some dust particles. Therefore, we washed them with distilled water. Then, they were dried in a fume hood for 24 h. The cleaned and dried leaves of *Quercus alba* were crushed and ground and passed through a sieve of 150 μm. A very fine biomass powder was further processed for the absorption step [28]. In this study, H_3PO_4 was used as the activating agent. The absorption time of the H_3PO_4 (wt 50%) activation agent was studied for 16 h, 24 h, 48 h, and 72 h. The material was calcined in a furnace at 500 °C for three h. The excess H_3PO_4 in the prepared char was removed by washing with distilled water until the pH remained neutral [11]. Finally, it was dried in an oven for 24 h at 105 °C to acquire activated carbon. The schematic diagram for the preparation of activated carbon is shown in Figure 2.
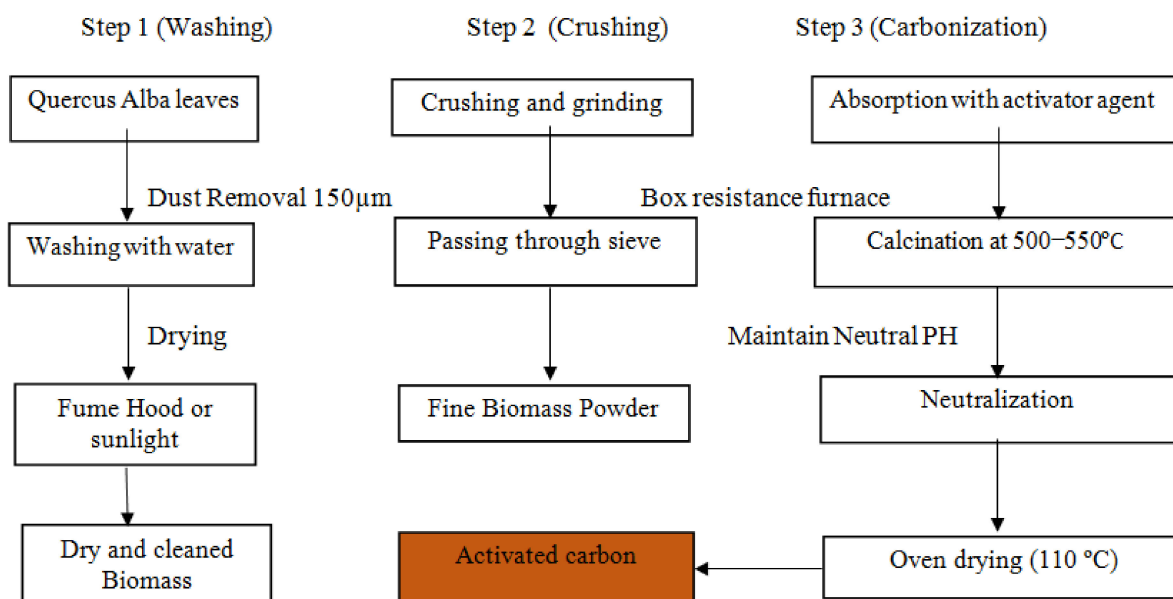
Figure 2. Preparation steps of activated carbon.

2.3. Characterization of Activated Carbon

A Micromeritics Gemini V Flow Prep 060 (Gemini V-060, Seoul, Korea) was used to analyze the surface area (S_{BET}). SEM–EDX (EM-30AX, COXIC2-17230 Model SPT-20,COXEM, Seoul, Korea) was used to reveal the surface morphology. Smart Lab (Rigaku, Japan) was used to determine the crystal structure (X-ray diffraction technique). A TENSOR-27 (Bruker, Germany) was used to determine the functional group of prepared activated carbon (FT-IR spectrum technique). Leco Model: 701 (Seoul, Korea) was used to analyze the thermal (TGA) behavior of the prepared activated carbon.

2.4. Life Cycle Assessment Compartments

In order to demonstrate significantly improved environmental performance, the compartments of LCA divided the process into four distinct steps.

2.5. Data Origin

The input/output data that were obtained were based on experiments involving AC production that were conducted at the lab scale. The existing framework includes processing waste material to obtain a final product. The disposal scenario of waste-based AC was excluded. The supply of resources, energy, and feedstock and their utilization were taken into consideration throughout the entire production process.

2.6. Goal and Scope Definition

The objective of this study was to produce one gram of AC as a functional unit from six grams of raw material, which extended the present study's scope, and the ecological implications were investigated.

2.7. System Boundary

A set of criteria called the system boundary was designed specifically for the eight steps of the AC production process: (1) raw material collection, (2) washing, (3) drying, (4) crushing and grinding, (5) H_3PO_4 impregnation, (6) calcination, (7) neutralization, and (8) drying the final material. The life cycle framework does not incorporate the storage of waste since it is apparent.

2.8. Life Cycle Assessment

LCA methodology was implemented using OpenLCA 1.10.3 software, while ReCiPe Midpoint (H) was used for environmental impact assessment. LCA involves optimizing or modifying the process steps to identify environmental in adequacies by incorporating alternative sources. Life cycle inventory analysis (LCI) includes product stages, processes, waste types, system descriptions, and variables to estimate the material utilized in the study. Within the framework of LCA, input/output energy flows and raw materials are considered in reference to functional unit adaptation. As per existing environmental regulations, life cycle impact assessment (LCIA) provides the computation settings and appropriate procedures [29]. Impact assessment aims to assess the efficiency and importance of the existing system using environmental indicators. Interpretation facilitates decision making, conclusions, and recommendations premised on preceding reports. Interpretation also encompasses regional ecological strategies. Table 1 shows the inventory data for one gram of laboratory-scale AC production from six grams of *Quercus alba*.

Table 1. Life cycle inventory of waste leaves of *Quercus alba* conversion to activated carbon.

Sample ID	Initial Biomass (Grams)	Grinding/Sieving		Chemical Activation		Washing/Oven Drying		Final AC (Grams)
ACQ-H-16	6	Power (kWh) H_2O (mL)	0.3 800	H_3PO_4 (mL) Power (kWh) H_2O (mL)	3 11.9 5.2	H_2O (mL) Filter paper Power (kWh)	1752 2 6	1
ACQ-H-24	6	Power (kWh) H_2O (mL)	0.3 800	H_3PO_4 (mL) Power (kWh) H_2O (mL)	3 11.9 5.2	H_2O (mL) Filter paper Power (kWh)	1841 2 6	1
ACQ-H-48	6	Power (kWh) H_2O (mL)	0.3 800	H_3PO_4 (mL) Power (kWh) H_2O (mL)	3 11.9 5.2	H_2O (mL) Filter paper Power (kWh)	2153 3 6	1
ACQ-H-72	6	Power (kWh) H_2O (mL)	0.3 800	H_3PO_4 (mL) Power (kWh) H_2O (mL)	3 11.9 5.2	H_2O (mL) Filter paper Power (kWh)	2756 4 6	1

3. Results and Discussion

3.1. Scanning Electron Microscopy Analysis (SEM)

The SEM images in Figure 3a,b show that the raw *Quercus alba* had heterogeneous particles with different shapes and different sizes. No pores were present in the structure of the raw precursors. Figure 3c reveals that pores were formed when H_3PO_4 was used as the activating agent. As shown in Figure 3c, when the absorption time of the activation agent was 16 h, the pores were enlarged due to the heat generated by the exothermic reaction between H_3PO_4 and water. The macropores seem to be connected to mesopores to form irregular pores. As the absorption time of phosphoric acid was increased to 24 h, 48 h, and 72 h, as shown in Figure 3d–f, the intensity of the heat caused by the exothermic reaction was reduced with the passage of time, and only a small number of mesopores were observed in the particle.
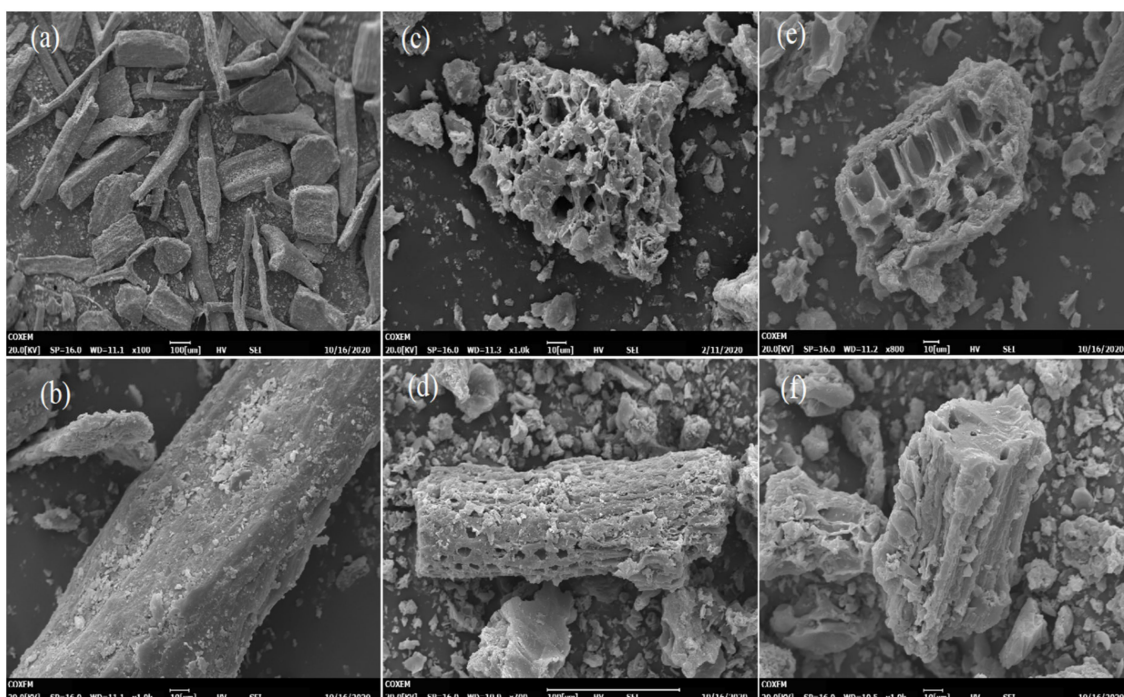
Figure 3. SEM micrographs of activated carbon (**a**,**b**) from raw *Quercus alba* (**c**) 16 h, (**d**) 24 h, (**e**) 48 h, and (**f**) 72 h using H_3PO_4.

3.2. EDX and BET Analysis

The change in the absorption time with H_3PO_4 chemical activation in Quercus reveals the change in carbon composition. The carbon content of *Quercus alba* was reduced as the absorption time of H_3PO_4 increased. The higher absorption time of H_3PO_4 was responsible for the reduced carbon composition. Carbon content decreased as the absorption time increased because with the passage of time, the exothermic reaction was fully accomplished [30]. The presence of oxygen in *Quercus alba* is due to the volatile compounds and their botanical species, such as furfural, decanal, vitispirane, terpineol, and nonamal [31].

The nutritional content of *Quercus alba* varies depending on the geographical location of the tree. It is mostly composed of protein, phosphoric acid, calcium, fat, fiber, and moisture content. The leaves have a calcium content that increases slowly as the growing season progresses. In the EDX analysis, *Quercus alba* and the prepared activated carbon showed a calcium presence due to the natural existence of calcium compounds [1]. In this study, the activated carbon was prepared at 500 °C. Calcium has a melting point of 842 °C. This is why the calcium was not fully evaporated and was still present in the activated carbon. For the complete removal of calcium from the activated carbon, a temperature of more than 842 °C is required. The presence of phosphoric acid is due to the use of H_3PO_4

as the activating agent. In addition, the results in Table 1 reveal that as the absorption time of the activation agent increased from 16 h to 72 h, the volume required for washing the biochar also increased. This indicates that as the absorption time of H_3PO_4 increased, more H_3PO_4 was absorbed into the sample, and a higher volume of water was required to maintain a neutral pH. Table 2 shows the EDX and BET results of the prepared activated carbon. In this study, the yield of the activated carbon prepared from the waste leaves of *Quercus alba* was roughly 17%. From 6 g of waste leaves of *Quercus alba*, 1 g of activated carbon was obtained.

Table 2. EDX and BET analysis of prepared AC.

Sample ID	Activation Time (h)	Pyrolysis Temperature (°C)	Pyrolysis Time (h)	Elements Presence (Weight %)				BET Surface Area m^2/g
				Carbon	Oxygen	Phosphor	Calcium	
Quercus alba				34.76	58.32	0.00	6.92	
ACQ-H-16	16	500	3	60.19	26.45	11.06	2.30	787.7
ACQ-H-24	24	500	3	53.32	29.41	13.15	4.12	890.2
ACQ-H-48	48	500	3	52.76	28.92	12.51	4.71	943.2
ACQ-H-72	72	500	3	54.56	30.02	12.00	3.43	896.4

3.3. X-Ray Diffraction Analysis

The XRD spectrum of the activated carbon prepared by H_3PO_4 is shown in Figure 4. Figure 4 shows peaks at 23°, signifying the presence of the crystalline carbonaceous structure of activated carbon [32]. One small peak at 15° was observed due to the turbostratic stacking of layers and the use of H_3PO_4 as the activating agent. A small peak at 43° further confirmed the presence of the crystalline carbonaceous structure of the activated carbon by using phosphoric acid [11,33].
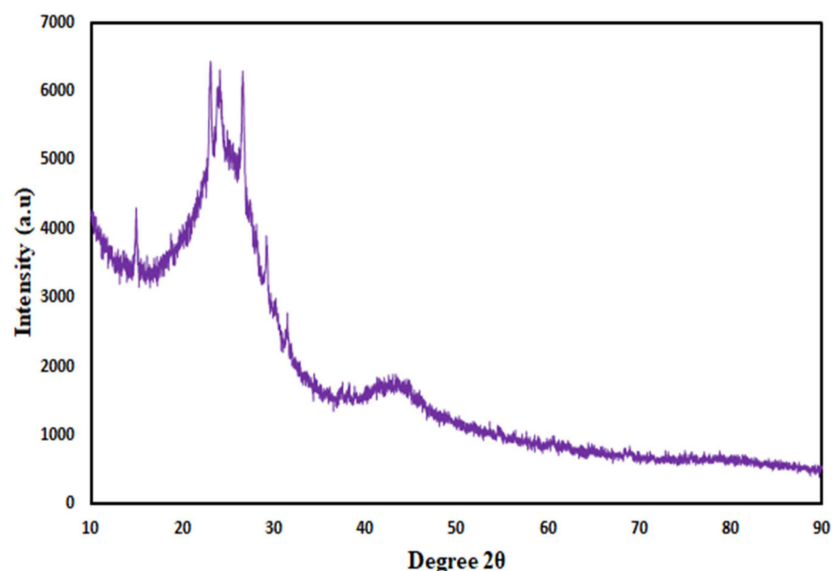
Figure 4. XRD analysis of activated carbon.

3.4. Thermogravimetric Analysis

The overall TGA analysis of *Quercus alba* by H_3PO_4 activation agents is shown in Figure 5. H_3PO_4 promotes the breaking of lignocellulose linkages, which results in the early development of volatile chemicals [34]. The result reveals that the H_3PO_4-based activated carbon started to degrade at 300 °C and was fully degraded above 875 °C. The

pore-forming mechanism of phosphoric acid is accomplished in the subsequent chemical reactions [35].

$$nH_3PO_4 \rightarrow 2P_nO_{3n+1} + H_n + (n-1)H_2O \tag{1}$$

$$2H_3PO_4 \rightarrow 3H_2O + P_2O_5 \tag{2}$$

$$2H_3PO_4 \rightarrow H_2O + H_2P_2O_7^{2-} + 2H^+ \tag{3}$$

$$2H_2P_2O_7^{2-} \rightarrow 6O_2 + P_4 + 2H_2O \tag{4}$$

$$2P_2O_5 + 5C \rightarrow P_4 + 5CO_2 \tag{5}$$

$$P_2O_5(liquid) \rightarrow P_2O_5(gas) \tag{6}$$
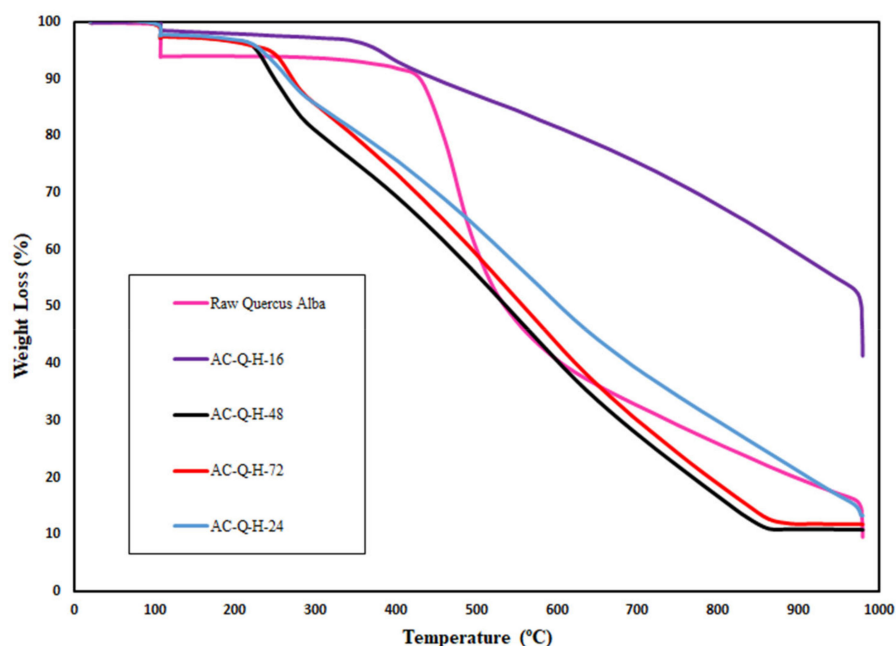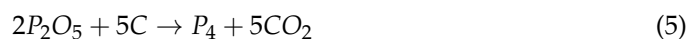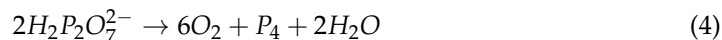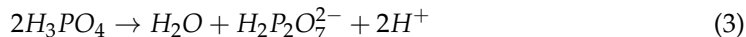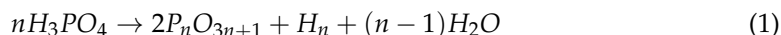
Figure 5. TGA analysis of activated carbon.

According to the TGA graph, the weight loss behavior of activated carbon prepared by H_3PO_4 activation had the same order as the BET surface area (Table 2). The weight loss value of the 16 h absorption time (AC-Q-H-16) at 550 °C was 15.44% (100-84.56), and the surface area was 787.7 m^2/g. The 24 h absorption time (AC-Q-H-24) had a weight loss value of 42.52% (100-57.48) and a surface area of 896.4 m^2/g. The 48 h H_3PO_4 absorption time (AC-Q-H-48) revealed the highest weight loss value of 51.74% (100-48.26), and the surface area was observed as 943.2 m^2/g. Finally, the 72 h absorption time (AC-Q-H-24) revealed a weight loss of 48.48% (100-51.52), and the surface area was 890.2 m^2/g.

3.5. FT-IR Analysis

The surface functional groups of the prepared activated carbon were analyzed by Fourier transform infrared spectroscopy (FT-IR), as shown in Figure 6. FT-IR analysis provides information on chemical bonds and decomposition and identifies the oxidation formations. The FT-IR results of H_3PO_4-based activated carbon revealed that bonds at wavenumbers of 1078 cm^{-1} and above 1100 cm^{-1} were attributed to C-O vibration. The presence of phosphorus and oxygen compounds (P-O-C) was observed at wavenumbers of 1200–1000 cm^{-1}, consistent with the elemental analysis results. In addition, the bond at 1565 was assigned to C=C vibration [35,36].A very weak peak at wavenumbers between 2300 and 3000 cm^{-1} was attributable to vibration in the alkyne group [28].
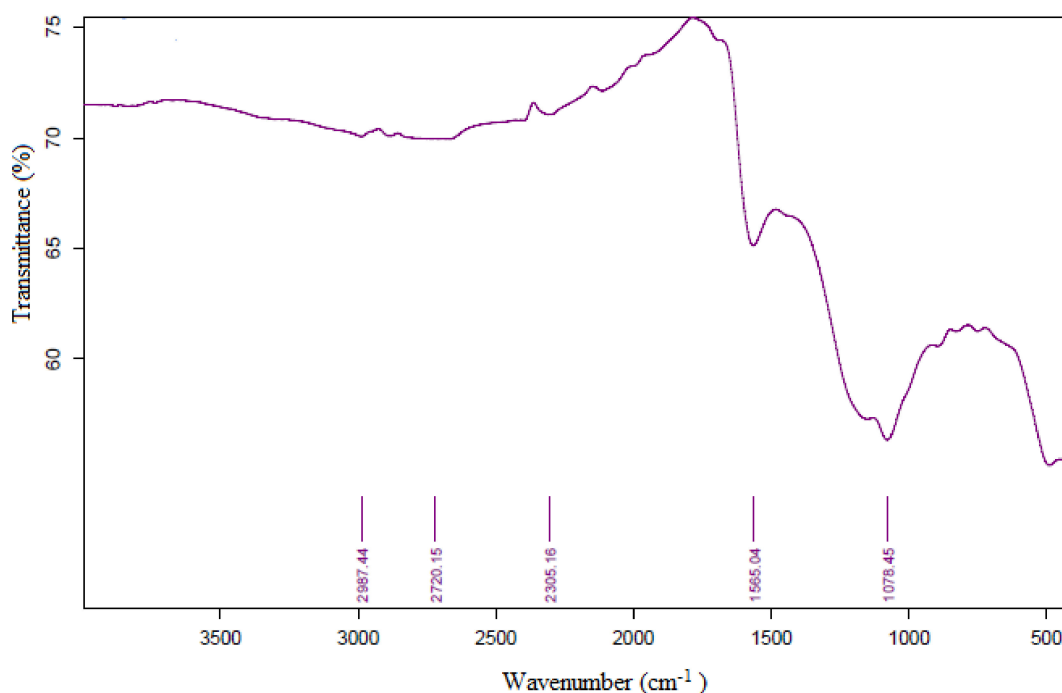
Figure 6. FT-IR analysis of activated carbon.

3.6. Environmental Impact Assessment

Table 3 depicts the characterized ReCiPe midpoint (H) impact categories for the 1 g of AC produced from 6 g of waste leaves of *Quercus alba*, while Figure 7 shows the normalized values of the AC production at the laboratory scale. The analyzed case study shows that the impact categories related to toxicity (TETP, HNTP, HCTP, FETP, and METP) were particularly affected. The utilization of electrical energy (which contributes on average $\approx 90\%$) was ultimately accountable for toxicity-related impact categories. Along with distilled water ($\approx 20\%$), electricity contributed $\approx 70\%$ of the FEP. Additionally, other impact indicators exhibiting lesser but still significant normalized impacts also emerged. However, with regard to Figure 8, the power utilized during laboratory procedures was the main cause of environmental impact, contributing an average of nearly 70% across all impact categories, with the maximum contribution to the impact category of freshwater ecotoxicity potential ($\approx 97\%$) and the minimum contribution to land use potential ($\approx 10\%$). Filter paper ($\approx 1.2\%$ overall), phosphoric acid ($\approx 1.4\%$ overall), and distilled water ($\approx 9\%$ overall) are other important contributors.

Table 3. Characterized ReCiPe Midpoint (H) impact categories for AC production from waste leaves of *Quercus alba* (FU: 1 g).

Impact Category	Value	Unit
(PMFP) Fine particulate matter formation potential	0.01	kg $PM_{2.5}$ eq
(FETP) Freshwater ecotoxicity potential	1.10	kg 1,4-DCB
(WCP) Water consumption potential	0.03	m^3
(IRP) Ionizing radiation potential	0.80	kBq Co-60 eq
(ODP) Stratospheric ozone depletion potential	0.00	kg CFC_{11} eq
(LUP) Land use potential	0.30	m^2 a crop eq
(METP) Marine ecotoxicity potential	1.35	kg 1,4-DCB
(MEP) Marine eutrophication potential	0.00	kg N eq
(TAP) Terrestrial acidification potential	0.02	kg SO_2 eq

Table 3. *Cont.*

Impact Category	Value	Unit
(OFTP) Ozone formation, Terrestrial ecosystem potential	0.01	kg NO$_x$ eq
(TETP) Terrestrial ecotoxicity potential	30.12	kg 1,4-DCB
(FSP) Fossil resource scarcity potential	1.18	kg oil eq
(GWP) Global warming potential	3.61	kg CO$_2$ eq
(FEP) Freshwater eutrophication potential	0.00	kg P eq
(MSP) Mineral resource scarcity potential	0.81	kg Cu eq
(OFHP) Ozone formation, Human health potential	0.01	kg NO$_x$ eq
(HNTP) Human non-carcinogenic toxicity potential	4.30	kg 1,4-DCB
(HCTP) Human carcinogenic toxicity potential	0.21	kg 1,4-DCB
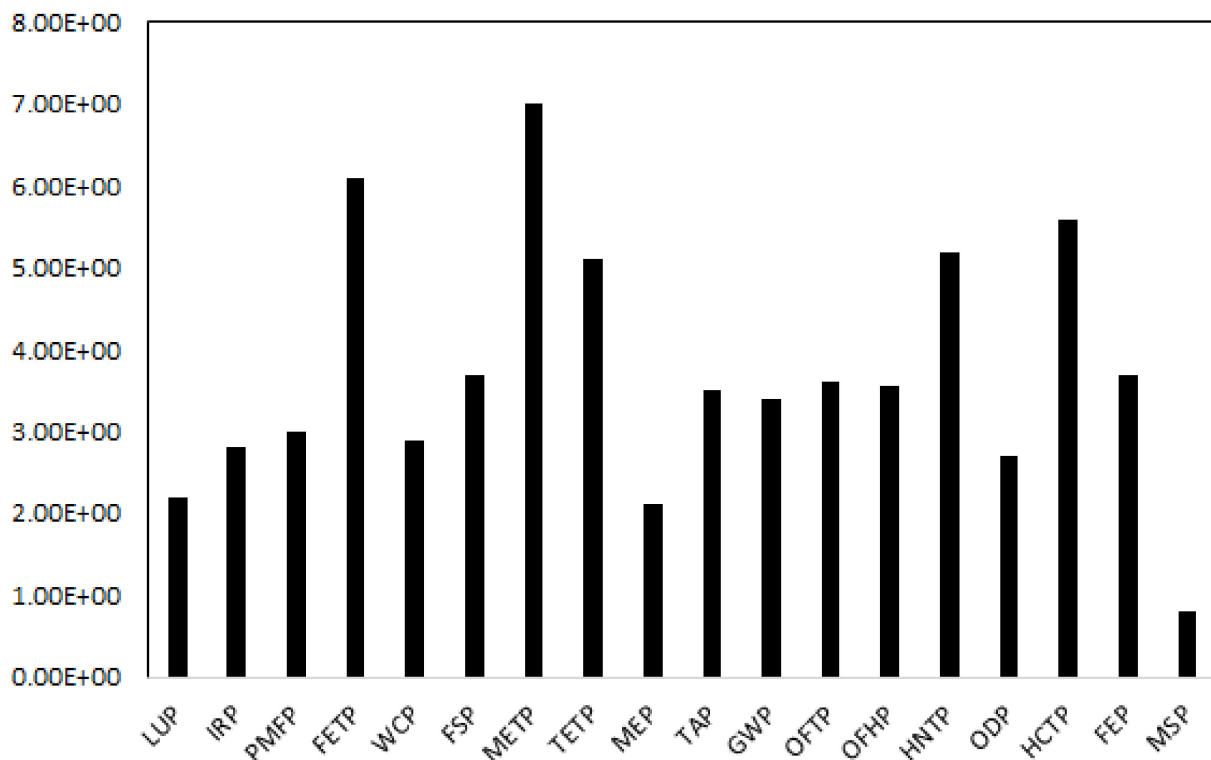
Figure 7. Normalized ReCiPe Midpoint (H) impact categories for AC production from waste leaves of *Quercus alba* (FU: 1 g).

The associated environmental impacts with different AC samples variegates because activated carbon can be produced by either chemical [37] or physical [24] activation from different carbonaceous materials or by combining the two methods. In this study, LCA was performed on the basis of life cycle inventory with predictive data [38], utilizing analytical determination and experimental measurements without uncertainty consideration in resource utilization and emissions. This is an analysis simplification because information about uncertainty is necessary to support conclusions based on the results of LCA [39]. It is important to appropriately manage the uncertainty in LCA since under a probabilistic methodology, various studies on the same production chain may produce contradictory conclusions, which could result in a poor decision-making process [40,41]. The incorporation of stochastic analysis is necessary when developing an LCA that involves uncertainty analysis. This kind of assessment is usually performed using Latin hypercube and Monte Carlo sampling techniques, which need a distribution of the probability of the critical

life cycle variables, e.g., energy consumption, chemical reagents, yield, flow, emissions, and adsorption capacity. However, it is not easy to incorporate uncertainty factors when producing AC using the LCA approach. This is because of the scarcity of information on the aforementioned parameters concerning the probability distribution in the literature. Hence, this gap in knowledge provides a potential opportunity in this area.
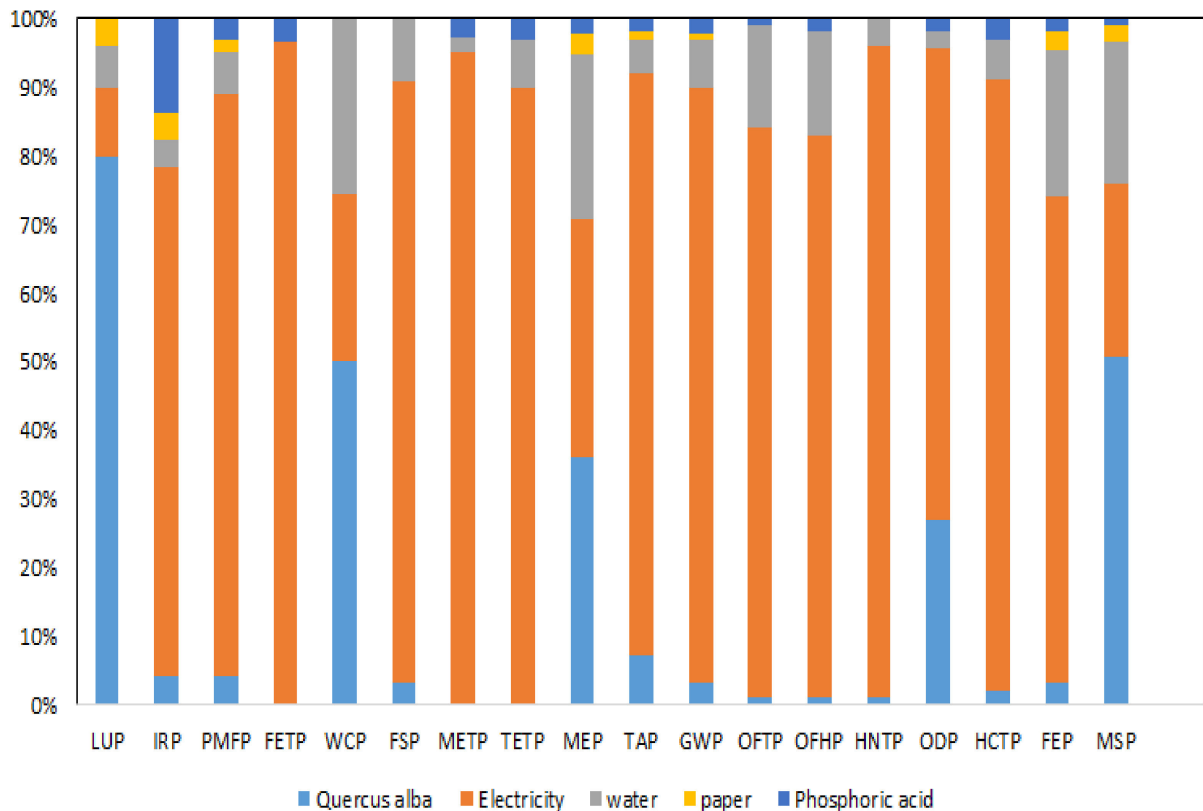

Figure 8. ReCiPe Midpoint (H) characterized percentage contribution of the AC production from waste leaves of *Quercus alba* (FU: 1 g).

Researchers [25] assessed the environmental impacts of AC production from cocoa pods using cradle-to-gate LCA methodology. The authors found that electricity consumption during the laboratory steps affected most of the selected impacts categories. The effect of GWP was 4.63 kg CO_2 eq, which was higher in this study. As most of the power used during laboratory-scale AC production comes from non-renewable sources, energy from renewable sources can reduce this effect. The authors concluded that power use during the laboratory steps affected most of the environmental impact categories. Another related study was conducted [9] using the steam activation method to produce AC from coconut shells at 900 °C. The authors found that electricity consumption during the laboratory steps affected most of the selected impact categories, particularly GWP and human toxicity. The authors also observed that the impacts of GWP and human toxicity were reduced significantly by using electrical energy from renewable sources.

Recently, researchers conducted gate-to-gate LCA for AC production from olive trees using H_3PO_4 as the activation agent. CML 2 baseline 2000 methodology was used for impact assessment, and OpenLCA 1.10.3 software was used for LCA modeling. The results showed that the impact of GWP and toxicity-related impact categories was higher (5.120 kg CO_2 eq and 3.262 kg 1,4-DCB) than those in this study, which indicates that *Quercus alba* is the most feasible material for AC production. Table 4 shows the results compared with those from the existing literature in terms of the most identified impact categories.

Table 4. Comparison of environmental impacts with existing literature.

Raw Material	Impact Categories	Value	Unit	References
Cocoa pods	Global warming potential	4.63	kg CO_2 eq	[25]
	Acidification Potential	0.03	kg SO_2 eq	
	Human Toxicity Potential	0.27 (carcinogenic)	kg 1,4-DCB	
		6.35 (non-carcinogenic)		
Coconut shells	Global warming potential	2.1×10^{-11} (normalized)	kg CO_2 eq	[24]
	Acidification Potential	4.1×10^{-11} (normalized)	kg SO_2 eq	
	Human Toxicity Potential	1.2×10^{-10} (normalized)	kg 1,4-DCB	
Olive tree	Global warming potential	5.210	kg CO_2 eq	[11]
	Acidification Potential	0.100	kg SO_2 eq	
	Human Toxicity Potential	3.262	kg 1,4-DCB	
Quercus alba	Global warming potential	3.61	kg CO_2 eq	This work
	Acidification Potential	0.02	kg SO_2 eq	
	Human Toxicity Potential	0.21 (carcinogenic)	kg 1,4-DCB	
		4.30 (non-carcinogenic)		

4. Conclusions

The activated carbon prepared from waste leaves of *Quercus alba* showed that when the absorption time of activating agent was increased, the surface increased. FT-IR analysis of H_3PO_4 revealed the oxygen and phosphorus functionalities on the activated carbon, consistent with the elemental analysis results. The different absorption time of the H_3PO_4 activating agent was considered an important parameter for enhancing the properties of the prepared activated carbon. As the absorption time of phosphoric acid increased, the surface area increased until 48 h and then started to decline. Life cycle assessment was carried out in order to quantify the ecological implications associated with the laboratory-scale activated carbon production from wasted tree leaves of *Quercus alba*. The results demonstrated that the power used during the laboratory steps was the main cause of most of the toxicity-related impact categories and contributed an average of nearly 70% across all impact categories. Additionally, the utilization of distilled water contributed ($\approx$9% overall), followed by phosphoric acid ($\approx$1.4% overall) and filter paper ($\approx$1.2% overall). In conclusion, controlling the key elemental process variables in AC manufacturing and the production process is not only important from an ecological and economic perspective, but it is also necessary for obtaining porous-structure carbon for water treatment and various other applications.

Author Contributions: Conceptualization, Formal analysis, Funding acquisition, Investigation, Methodology, Project administration, Resources, Visualization, Writing—original draft, Writing—review and editing, M.A. and H.H.S. All authors have read and agreed to the published version of the manuscript.

Institutional Review Board Statement: Not applicable.

Informed Consent Statement: Not applicable.

Data Availability Statement: The data are presented in the present research article.

Conflicts of Interest: The authors declare no conflict of interest.

References

1. Tirmenstein, D.A. *Quercus alba*. In Fire Effects Information System. Available online: https://www.fs.usda.gov/database/feis/plants/tree/quealb/all.html (accessed on 22 October 2022).

2. Rogers, R. *Quercus alba* L. Available online: https://www.srs.fs.usda.gov/pubs/misc/ag_654/volume_2/quercus/alba.htm (accessed on 22 October 2022).

3. Thakur, A. Oak of India—Regenaration and Management. Available online: https://ifsa.net/oaks-of-india-regeneration-management/ (accessed on 22 October 2022).

4. Zhang, L.; Ding, W.; Zhou, G.; Wen, S.; Yin, J.; Liu, C.; Fu, Y. Two-Dimensional Activated Carbon Nanosheets from Natural Corn Straw Piths and its Rapid Removal of Tetracycline Via Strong Π-Π Electron Donor Receptor Interactions. *SSRN Electron. J.* **2022**, *360*, 127544. [CrossRef]

5. Hu, H.; Qu, J.; Yang, K.-R.; Hao, J.; Yang, J.; Song, R.-F.; Zhang, L.-Y.; Li, Z.-X. Tuning Carbon Contents and Further Capacitances of Coordination Polymer-Derived Carbonaceous Composites by Annealing Temperatures. *Cryst. Growth Des.* **2022**, *22*, 4503–4512. [CrossRef]

6. Bicil, Z.; Doğan, M. Characterization of Activated Carbons Prepared from Almond Shells and Their Hydrogen Storage Properties. *Energy Fuels* **2021**, *35*, 10227–10240. [CrossRef]

7. Elanthamilan, E.; Catherin Meena, B.; Renuka, N.; Santhiya, M.; George, J.; Kanimozhi, E.P.; Christy Ezhilarasi, J.; Princy Merlin, J. Walnut shell derived mesoporous activated carbon for high performance electrical double layer capacitors. *J. Electroanal. Chem.* **2021**, *901*, 115762. [CrossRef]

8. Keppetipola, N.M.; Dissanayake, M.; Dissanayake, P.; Karunarathne, B.; Dourges, M.A.; Talaga, D.; Servant, L.; Olivier, C.; Toupance, T.; Uchida, S.; et al. Graphite-type activated carbon from coconut shell: A natural source for eco-friendly non-volatile storage devices. *RSC Adv.* **2021**, *11*, 2854–2865. [CrossRef] [PubMed]

9. Ouzzine, M.; Serafin, J.; Sreńscek-Nazzal, J. Single step preparation of activated biocarbons derived from pomegranate peels and their CO2 adsorption performance. *J. Anal. Appl. Pyrolysis* **2021**, *160*, 11–17. [CrossRef]

10. Khader, E.H.; Mohammed, T.J.; Albayati, T.M. Comparative performance between rice husk and granular activated carbon for the removal of azo tartrazine dye from aqueous solution. *Desalin. Water Treat.* **2021**, *229*, 372–383. [CrossRef]

11. Amin, M.; Shah, H.H.; Iqbal, A.; Farooqi, Z.U.R.; Krawczuk, M.; Zia, A. Conversion of Waste Biomass into Activated Carbon and Evaluation of Environmental Consequences Using Life Cycle Assessment. *Appl. Sci.* **2022**, *12*, 5741. [CrossRef]

12. Daiem, M.M.A.; Rashad, A.M.; Said, N.; Abdel-Gawwad, H.A. An initial study about the effect of activated carbon nano-sheets from residual biomass of olive trees pellets on the properties of alkali-activated slag pastes. *J. Build. Eng.* **2021**, *44*, 102661. [CrossRef]

13. Eddy, N.O.; Ibok, U.J.; Garg, R.; Garg, R.; Iqbal, A.; Amin, M.; Mustafa, F.; Egilmez, M.; Galal, A.M. A Brief Review on Fruit and Vegetable Extracts as Corrosion Inhibitors in Acidic Environments. *Molecules* **2022**, *27*, 2991. [CrossRef] [PubMed]

14. Oliveira, L.C.A.; Pereira, E.; Guimaraes, I.R.; Vallone, A.; Pereira, M.; Mesquita, J.P.; Sapag, K. Preparation of activated carbons from coffee husks utilizing FeCl3 and ZnCl2 as activating agents. *J. Hazard. Mater.* **2009**, *165*, 87–94. [CrossRef]

15. Amin, M.; Munir, S.; Iqbal, N.; Wabaidur, S.M.; Iqbal, A. The Conversion of Waste Biomass into Carbon-Supported Iron Catalyst for Syngas to Clean Liquid Fuel Production. *Catalysts* **2022**, *12*, 1234. [CrossRef]

16. Rashidi, N.A.; Chai, Y.H.; Ismail, I.S.; Othman, M.F.H.; Yusup, S. Biomass as activated carbon precursor and potential in supercapacitor applications. *Biomass Convers. Biorefinery* **2022**, *913*, 0123456789. [CrossRef]

17. Sieradzka, M.; Kirczuk, C.; Kalemba-rec, I.; Mlonka-mędrala, A.; Magdziarz, A. Pyrolysis of Biomass Wastes into Carbon Materials. *Energies* **2022**, *15*, 1941. [CrossRef]

18. Phainuphong, S.; Taweekun, J.; Maliwan, K.; Theppaya, T.; Reza, S.; Azad, A.K. Synthesis and Characterization of Activated Carbon Derived from Rubberwood Sawdust via Carbonization and Chemical Activation as Electrode Material for Supercapacitor. *J. Adv. Res. Fluid Mech. Therm. Sci.* **2022**, *94*, 61–76. [CrossRef]

19. Mokrzycki, J.; Magdziarz, A.; Rutkowski, P. Biomass and Bioenergy The influence of the Miscanthus giganteus pyrolysis temperature on the application of obtained biochars as solid biofuels and precursors of high surface area activated carbons. *Biomass Bioenergy* **2021**, *164*, 106550. [CrossRef]

20. Heidarinejad, Z.; Dehghani, M.H.; Heidari, M.; Javedan, G.; Ali, I.; Sillanpää, M. Methods for preparation and activation of activated carbon: A review. *Environ. Chem. Lett.* **2020**, *18*, 393–415. [CrossRef]

21. Zou, R.; Qian, M.; Wang, C.; Mateo, W.; Wang, Y.; Dai, L.; Lin, X.; Zhao, Y.; Huo, E.; Wang, L.; et al. Biochar: From by-products of agro-industrial lignocellulosic waste to tailored carbon-based catalysts for biomass thermochemical conversions. *Chem. Eng. J.* **2021**, *441*, 135972. [CrossRef]

22. Khalil, K.M.S.; Elhamdy, W.A.; Mohammed, K.M.H.; Said, A.E.A.A. Nanostructured P-doped activated carbon with improved mesoporous texture derived from biomass for enhanced adsorption of industrial cationic dye contaminants. *Mater. Chem. Phys.* **2022**, *282*, 125881. [CrossRef]

23. Ahmad, A.A.; Al-Raggad, M.; Shareef, N. Production of activated carbon derived from agricultural by-products via microwave-induced chemical activation: A review. *Carbon Lett.* **2021**, *31*, 957–971. [CrossRef]

24. Arena, N.; Lee, J.; Clift, R. Life Cycle Assessment of activated carbon production from coconut shells. *J. Clean. Prod.* **2016**, *125*, 68–77. [CrossRef]

25. Tiegam, R.F.T.; Tchuifon, D.R.T.; Santagata, R.; Nanssou, P.A.K.; Anagho, S.G.; Ionel, I.; Ulgiati, S. Production of activated carbon from cocoa pods: Investigating benefits and environmental impacts through analytical chemistry techniques and life cycle assessment. *J. Clean. Prod.* **2021**, *288*, 125464. [CrossRef]

26. Ur, Z.; Farooqi, R.; Ahmad, I.; Ditta, A.; Ilic, P.; Amin, M. Types, sources, socioeconomic impacts, and control strategies of environmental noise: A review. *Environ. Sci. Pollut. Res.* **2022**, *94*, 0123456789. [CrossRef]

27. Sepúlveda-Cervantes, C.V.; Soto-Regalado, E.; Rivas-García, P.; Loredo-Cancino, M.; Cerino-Córdova, F.d.J.; Reyes, R.B.G. Technical-environmental optimisation of the activated carbon production of an agroindustrial waste by means response surface and life cycle assessment. *Waste Manag. Res.* **2018**, *36*, 121–130. [CrossRef] [PubMed]

28. Amin, M.; Chung, E.; Shah, H.H. Effect of different activation agents for activated carbon preparation through characterization and life cycle assessen. *Int. J. Environ. Sci. Technol.* **2022**, *78*, 0123456789. [CrossRef]

29. Yu, S.; Tao, J. Simulation based life cycle assessment of airborne emissions of biomass-based ethanol products from different feedstock planting areas in China. *J. Clean. Prod.* **2009**, *17*, 501–506. [CrossRef]

30. Lahmer, K. Numerical investigation of thermal and electrical management during hydrogen reversible solid- state storage using a novel heat exchanger based on thermoelectric modules. *Int. J. Hydrogen Energy* **2022**, *47*, 30580–30591. [CrossRef]

31. Gombau, J.; Cabanillas, P.; Mena, A.; Pérez-Navarro, J.; Ramos, J.; Torner, A.; Fort, F.; Gómez-Alonso, S.; García-Romero, E.; Canals, J.M.; et al. Comparative study of volatile substances and ellagitannins released into wine by *Quercus pyrenaica*, *Quercus petraea* and *Quercus alba* barrels. *OENO One* **2022**, *56*, 5551.

32. Xu, J.; Chen, L.; Qu, H.; Jiao, Y.; Xie, J.; Xing, G. Preparation and characterization of activated carbon from reedy grass leaves by chemical activation with H3PO4. *Appl. Surf. Sci.* **2014**, *320*, 674–680. [CrossRef]

33. Mahmood, S.; Iqbal, A.; Rafi-u-Din; Wadood, A.; Mateen, A.; Amin, M.; Yahia, I.S.; Zahran, H.Y. Influence of Homogenizing Methodology on Mechanical and Tribological Performance of Powder Metallurgy Processed Titanium Composites Reinforced by Graphene Nanoplatelets. *Molecules* **2022**, *27*, 2666. [CrossRef]

34. Gao, Y.; Yue, Q.; Gao, B.; Li, A. Insight into activated carbon from different kinds of chemical activating agents: A review. *Sci. Total Environ.* **2020**, *746*, 141094. [CrossRef] [PubMed]

35. Liu, Y.; Yap, X.; Wang, Z.; Li, H.; Shen, X.; Yao, Z.; Qian, F. Synthesis of Activated Carbon from Citric Acid Residue by Phosphoric Acid Activation for the Removal of Chemical Oxygen Demand from Sugar-Containing Wastewater. *Environ. Eng. Sci.* **2019**, *36*, 656–666. [CrossRef]

36. Shi, Y.; Liu, G.; Wang, L.; Zhang, H. Activated carbons derived from hydrothermal impregnation of sucrose with phosphoric acid: Remarkable adsorbents for sulfamethoxazole removal. *RSC Adv.* **2019**, *31*, 17841–17851. [CrossRef] [PubMed]

37. Hjaila, K.; Baccar, R.; Sarrà, M.; Gasol, C.M.; Bláquezn, P. Environmental impact associated with activated carbon preparation from olive-waste cake via life cycle assessment from olive-waste cake via life cycle assessment. *J. Environ. Manag.* **2013**, *130*, 242–247. [CrossRef] [PubMed]

38. Amin, M.; Shah, H.H.; Fareed, A.G.; Khan, W.U.; Chung, E.; Zia, A.; Rahman Farooqi, Z.U.; Lee, C. Hydrogen production through renewable and non-renewable energy processes and their impact on climate change. *Int. J. Hydrogen Energy* **2022**, *47*, 33112–33134. [CrossRef]

39. UNEP. Global Guidance Principles for Life Cycle Assessment Databases. Shonan Guid. Princ. 2010, p. 160. Available online: www.unep.org (accessed on 22 October 2022).

40. Huijbregts, M.A.J.; Gilijamse, W.; Ragas, A.M.J.; Reijnders, L. Evaluating uncertainty in environmental life-cycle assessment. A case study comparing two insulation options for a Dutch one-family dwelling. *Environ. Sci. Technol.* **2003**, *37*, 2600–2608. [CrossRef]

41. Hong, J.; Shaked, S.; Rosenbaum, R.K.; Jolliet, O. Analytical uncertainty propagation in life cycle inventory and impact assessment: Application to an automobile front panel. *Int. J. Life Cycle Assess.* **2010**, *15*, 499–510. [CrossRef]